Satellite earth observation as a tool to conceptualize hydrogeological fluxes in the Sandveld, South Africa

Zahn Műnch · Julian E. Conrad · Lesley A. Gibson · Anthony R. Palmer · Denis Hughes

Abstract In semi-arid, groundwater-dependent regions of South Africa, allocation of additional water resources can become problematic in the absence of quantified regional groundwater recharge values. In this study in the northern Sandveld, remote-sensing-data products for precipitation (P) and evapotranspiration (ET) are used to quantify groundwater recharge and guide the conceptualization of the hydrogeology of the study area. Data from three ET models (ET_{MODIS}, MOD16, Pitman rainfall-runoff) are compared; these models concur best in years of average rainfall, with model results deviating up to 30% in wet years. The MODIS data product (MOD16) is used in conjunction with gridded precipitation data to calculate spatial regional recharge. The long-term precipitation minus evapotranspiration (P–ET) budget closes on a positive 13±25%; however, when correcting ET (20% underestimation determined using the chloride mass balance method), the catchment average potential recharge is reduced to −4±30%. The use of P–ET clearly identifies potential recharge zones at higher elevation and discharge zones, highlighting irrigated agriculture. The usefulness of identifying recharge zones is demonstrated in the value added to conceptualizing the hydrogeology. Since some uncertainty around the accuracy of ET data still remains, it is recommended that the MODIS data product be validated more comprehensively in semi-arid environments.

Keywords South Africa · Groundwater recharge · Water balance · Remote sensing · Evapotranspiration · Conceptual models

Z. Műnch (✉)
CGA-Centre for Geographical Analysis,
Stellenbosch University,
Private Bag X/1, Matieland, 7602, South Africa
e-mail: zmunch@sun.ac.za

J. E. Conrad · L. A. Gibson
GEOSS-Geohydrological and Spatial Solutions International (Pty) Ltd, P.O. Box 12412, Die Boord, 7613, South Africa

J. E. Conrad
e-mail: jconrad@geoss.co.za

L. A. Gibson
e-mail: lgibson@geoss.co.za

A. R. Palmer
Centre for African Conservation Ecology,
Nelson Mandela Metropolitan University, P.O. Box 77000,
Port Elizabeth, 6031, South Africa
e-mail: Palmert@arc.agric.za

D. Hughes
Institute for Water Research,
Rhodes University, P.O. Box 94, Grahamstown, 6140, South Africa
e-mail: D.Hughes@ru.ac.za

Introduction

In South Africa's semi-arid regions, where there is reliance on groundwater for domestic and agricultural use, allocation of this resource has become an important political, legal, economic and environmental concern. The South African National Water Act (Act 36 of 1998) which undertakes to provide sustainable use of water for the benefit of all users also dictates that the ecological water requirements are satisfied before new water licenses are granted to other uses. The spirit of the Act is to achieve equitable distribution of water resources while including an allocation to the environment. The northern Sandveld, located on the Cape West Coast of South Africa, is characterized by low rainfall and minimal river flows and yet hosts significant aquifer systems (CapeNature 2006). The demands placed on groundwater within the area are substantial (GEOSS 2006) as groundwater supports extensive agriculture as well as domestic water supply. Furthermore, groundwater plays an important role in supporting a number of sensitive and unique ecosystems. Climate variability and the threat of climate change imply a decreasing certainty in rainfall and temperature patterns, emphasizing the need for water-resource managers to have accurate information about all aspects of water-resource occurrence and use.

The availability of several remote-sensing products has influenced the way in which water resources can be assessed and managed. Despite the fact that groundwater,

as a subsurface resource cannot be directly measured, but is generally inferred from more easily measurable physical and chemical parameters (Healy 2010; Scanlon et al. 2002), remote-sensing techniques have been used for exploration and assessment of groundwater resources, estimation of natural recharge distribution (Ahmad et al. 2005; Brunner et al. 2004; Klock and Udluft 2002), and hydrogeological data analysis, modelling, monitoring and management (Allen et al. 2005; Brunner et al. 2007; Crosbie et al. 2010a, b; Hendricks-Franssen et al. 2008; Hoffman 2005). Remote sensing has the general advantage of providing a spatially distributed measurement on a temporal basis. Remote-sensing data can be used to quantify recharge, water use and vegetation response (Allen et al. 2005; Bastiaanssen and Hellegers 2007) as part of sustainable groundwater exploitation by using relationships that exist within the water balance. The development of sustainable groundwater-resource programmes in data-poor semi-arid regions is dependent on knowledge of recharge rates particularly due to the erratic nature of recharge (Cook et al. 1989; Hendricks-Franssen et al. 2008) and the large uncertainties associated with recharge rates (Scanlon et al. 2006).

The water-balance equation for long-term averaged steady-state conditions can be reduced such that recharge can be calculated from precipitation (P) and evapotranspiration (ET) (Brunner et al. 2004; Szilagyi et al. 2011, 2012). In semi-arid regions, P and ET are very similar in magnitude and in calculating absolute values for P and ET there is a large associated error (Brunner et al. 2004, 2007; Glenn et al. 2011; Szilagyi et al. 2011, 2012). Therefore, quantification of recharge using this method may be prone to large errors and uncertainties but a precipitation minus evapotranspiration (P–ET) difference map can be used to identify distinct zones of recharge (Brunner et al. 2004, 2007; Hendricks-Franssen et al. 2008). The term recharge may be used to describe potential recharge, gross recharge or net recharge as defined by Crosbie et al. (2010a).

Following Brunner et al. (2004), it will be demonstrated in this paper how P and ET derived from earth observation data can be used as a tool for the conceptualization of groundwater fluxes in a semi-arid catchment. The approach is based on catchment average values for a quaternary catchment to determine whether the outflows exceed the inflows. Within-catchment P–ET results will be used to corroborate and extend on the hydrogeological conceptualization of the catchment described in the literature. The approach relies on the use of available remote-sensing data products thereby reducing the length of the data processing chain. The results of this study lead to the recommendation that these technologies are considered as aids for conceptualizing hydrogeological fluxes particularly in ungauged catchments.

Study area

For complex heterogeneous landscapes, there is lower confidence in variables such as biophysical parameters derived from low-resolution sensor data (Gibson et al. 2011a) and the corollary is therefore that for homogeneous catchments there is a higher confidence in retrieved biophysical parameters. In South Africa, the quaternary catchment is the basic water-resource management unit; and 1,946 such catchments have been demarcated (Midgley et al. 1994), nested within tertiary, secondary and primary drainage areas, each represented by a letter and number making up a four-letter name, having similar runoff volumes. G30G represents a catchment in the Sandveld region (G3) of the Olifants-Doorn water-management area (G) with each character denoting primary (G), secondary (G3), tertiary (G30) and quaternary (G30G) sub-catchments respectively. A statistical analysis of the quaternary catchments in the Sandveld revealed that G30G represented a relatively homogeneous catchment within the Sandveld (Gibson et al. 2011b). The complexity of the study area was determined by the distribution of mapped landcover classes (van den Berg et al. 2008) within a 1 km^2 MODIS pixel indicating that approximately 60 % of the catchment consists of MODIS pixels with homogeneous landcover confirming the suitability of G30G to illustrate the use of MODIS resolution remote-sensing products for the Sandveld region.

G30G (647 km^2 in area) is located in the northern Sandveld about 300 km north of Cape Town (Fig. 1a). The upper reaches of the catchment comprise mountainous and rugged terrain at median elevation of 580 m above mean sea level (amsl). Near the town of Graafwater (Fig. 1b) the topography becomes flatter to the west with subdued topographical variation. The transition from mountainous area to flatter-lying, sand-covered topography occurs at an elevation of approximately 250 m amsl. The Jakkals River is a small seasonal system which experiences zero flow for more than 33 % of the year (DWAF 2011) and terminates in the Jakkalsvlei coastal lake at Lamberts Bay. G30G receives approximately 253 mm/a rainfall and falls within a winter rainfall region (Middleton and Bailey 2008). The lowest and highest rainfall typically occurs in January and June respectively (Fig. 2), while the warmest and coldest months, January and July, record minimum and maximum temperatures ranging from long-term averages of 14 and 29 °C and 6 and 18 °C respectively (Schulze and Lynch 2007).

The catchment contains large agricultural areas. It is estimated that the agricultural sector abstracts 6,900 m^3/ha/a for irrigation from groundwater—mainly for potato crops (GEOSS 2006). Up until 2007, the total area cleared for potato crops in G30G was 2 963 ha, with 1,042 ha planted, decreasing to 1,011 ha in 2011. Additional groundwater is abstracted for domestic water supply for the town of Graafwater with abstraction figures for 2005 totalling 0.16×10^6 m^3, with the demand for summer months double that of demand in winter (GEOSS 2006). Although Lamberts Bay is also dependent on groundwater for domestic supply purposes, the water is imported from outside the catchment. Figure 3 illustrates the dominant landcover and agricultural development.
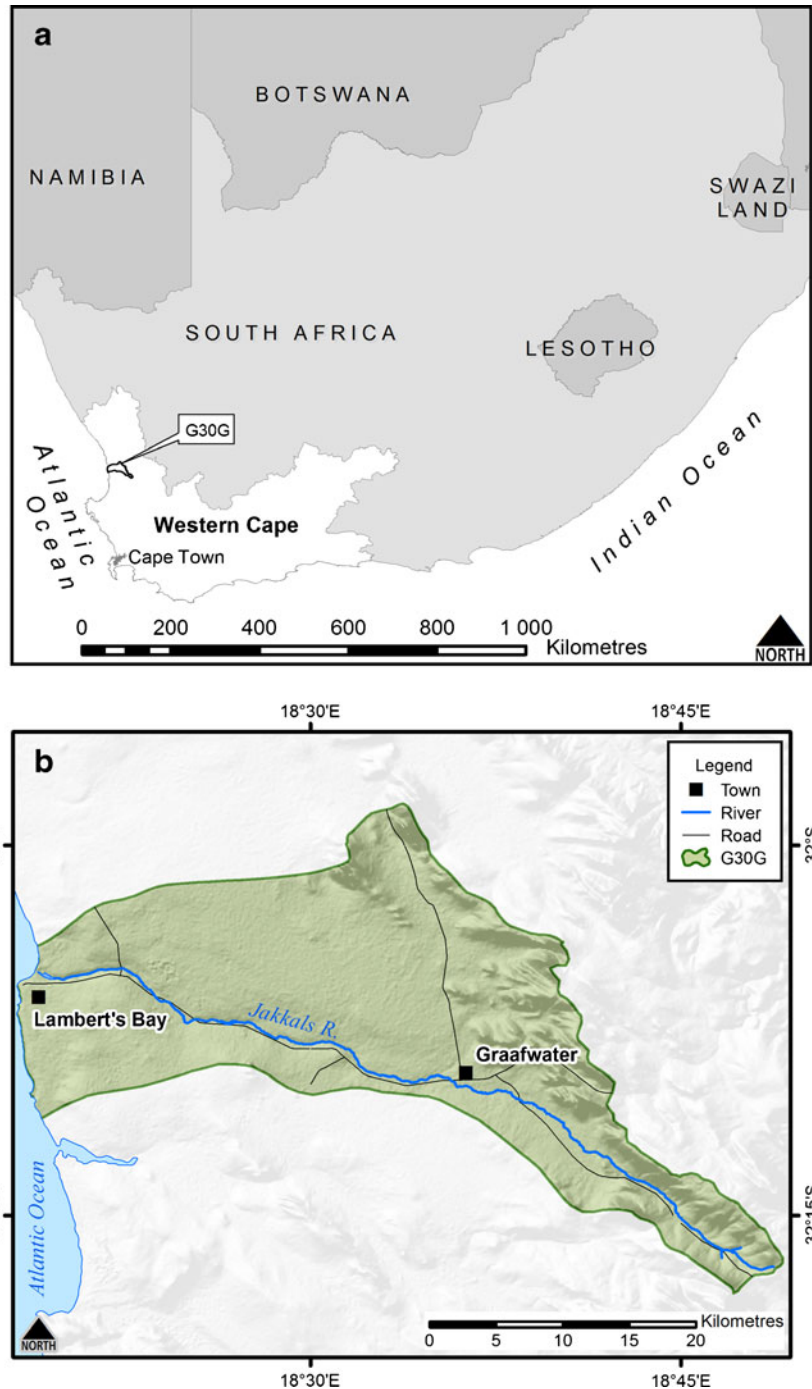
Fig. 1 **a** Location of the study area, quaternary catchment G30G with **b** main towns and rivers

The vegetation of the catchment is mainly characterized as shrubland and fynbos in Fig. 3. The inland portion of G30G is predominantly Leipoldtville Sand Fynbos (50.4 %; Mucina and Rutherford 2006), a shrubland with an open stratum of emergent, tall (2–3 m) shrubs in clumps. Lamberts Bay Strandveld (26 %), located close to the coast, comprises medium-height (1.2–1.5 m), dense evergreen and drought-deciduous shrubs, with a dense understory of low (0.2–0.5 m) unpalatable shrubs. In the inland mountainous regions, low scrub and scattered tall shrubs of the Graafwater Sandstone Fynbos (20.6 %) are found. Also present in the catchment are

several azonal vegetation types including Cape Seashore Vegetation, Cape Estuarine Salt Marshes and Cederberg Sandstone Fynbos (Mucina and Rutherford 2006).

Geological and hydrogeological setting

The geological setting of G30G is provided in Fig. 4 (de Beer 2003). Most of the catchment is underlain by a variable thickness of Table Mountain Group (TMG) rocks, part of the Cape Supergroup, dominated by thick quartzose sandstones,
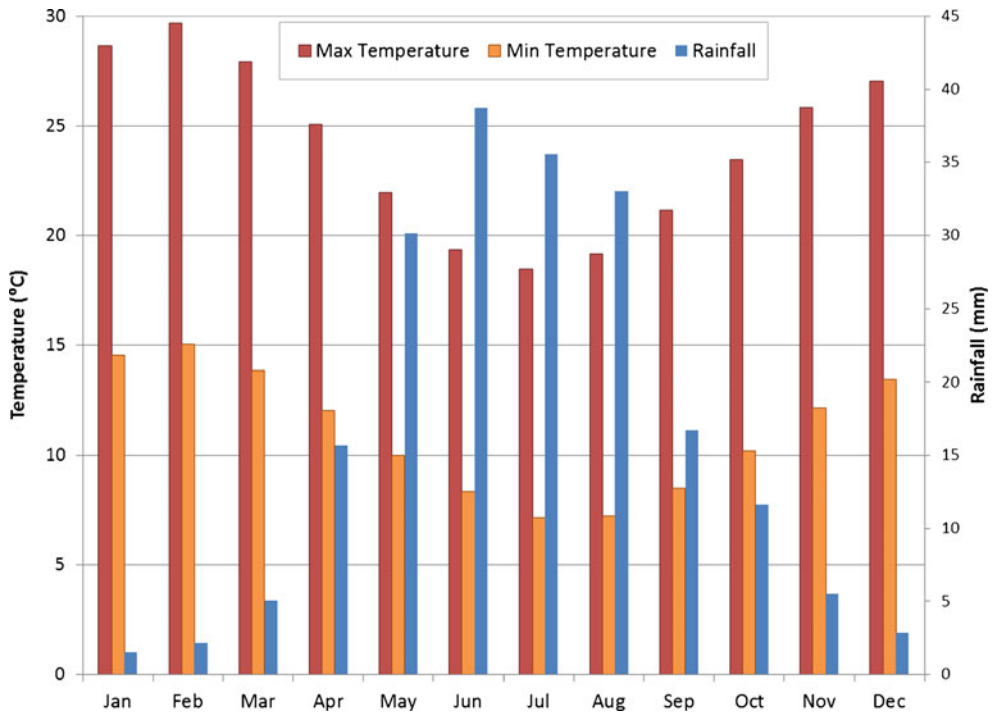
Fig. 2 Long-term average rainfall, and maximum and minimum temperatures for catchment G30G (after Schulze and Lynch 2007)
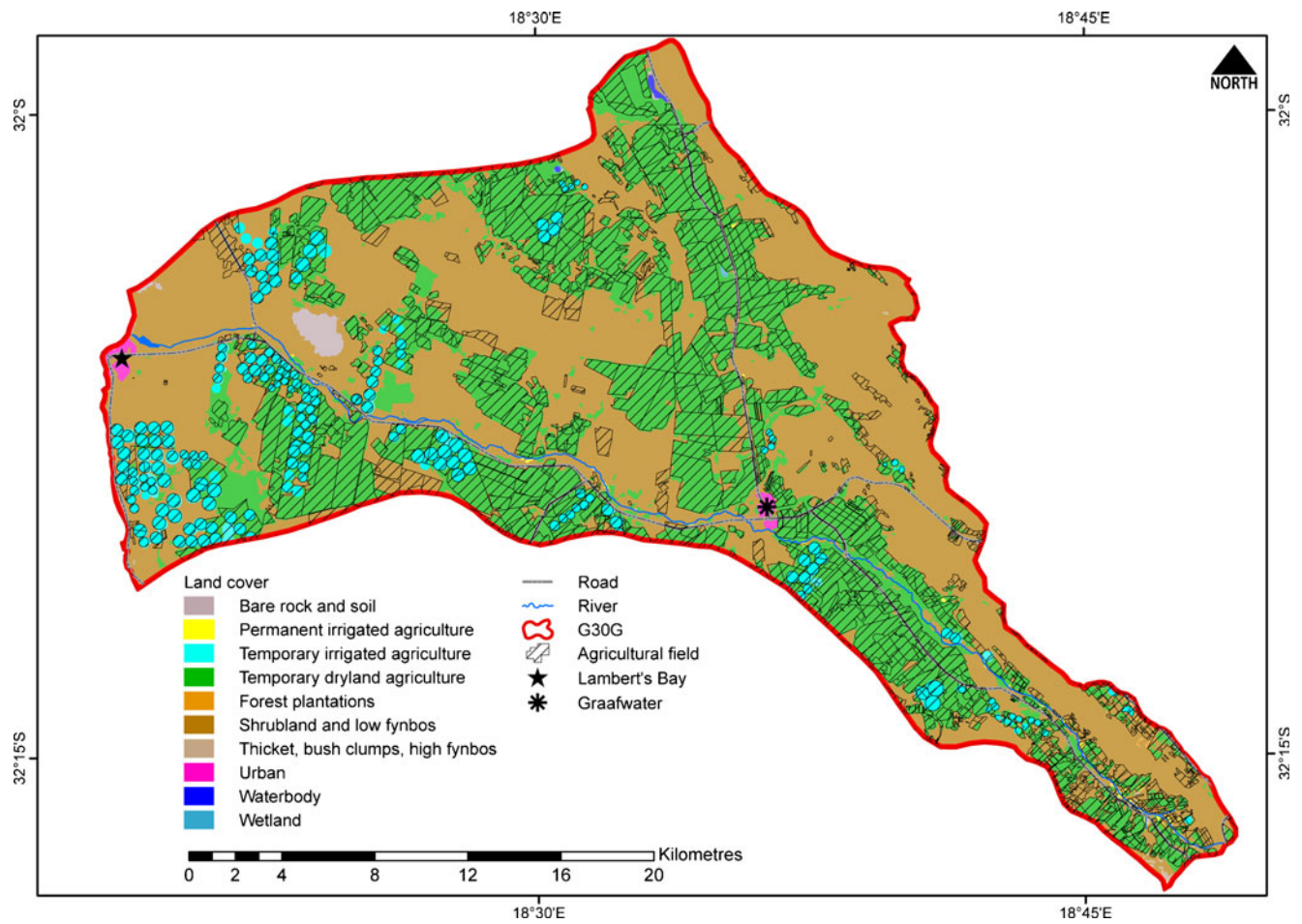

Fig. 3 Landcover (after van den Berg et al. 2008) and agricultural fields of G30G catchment
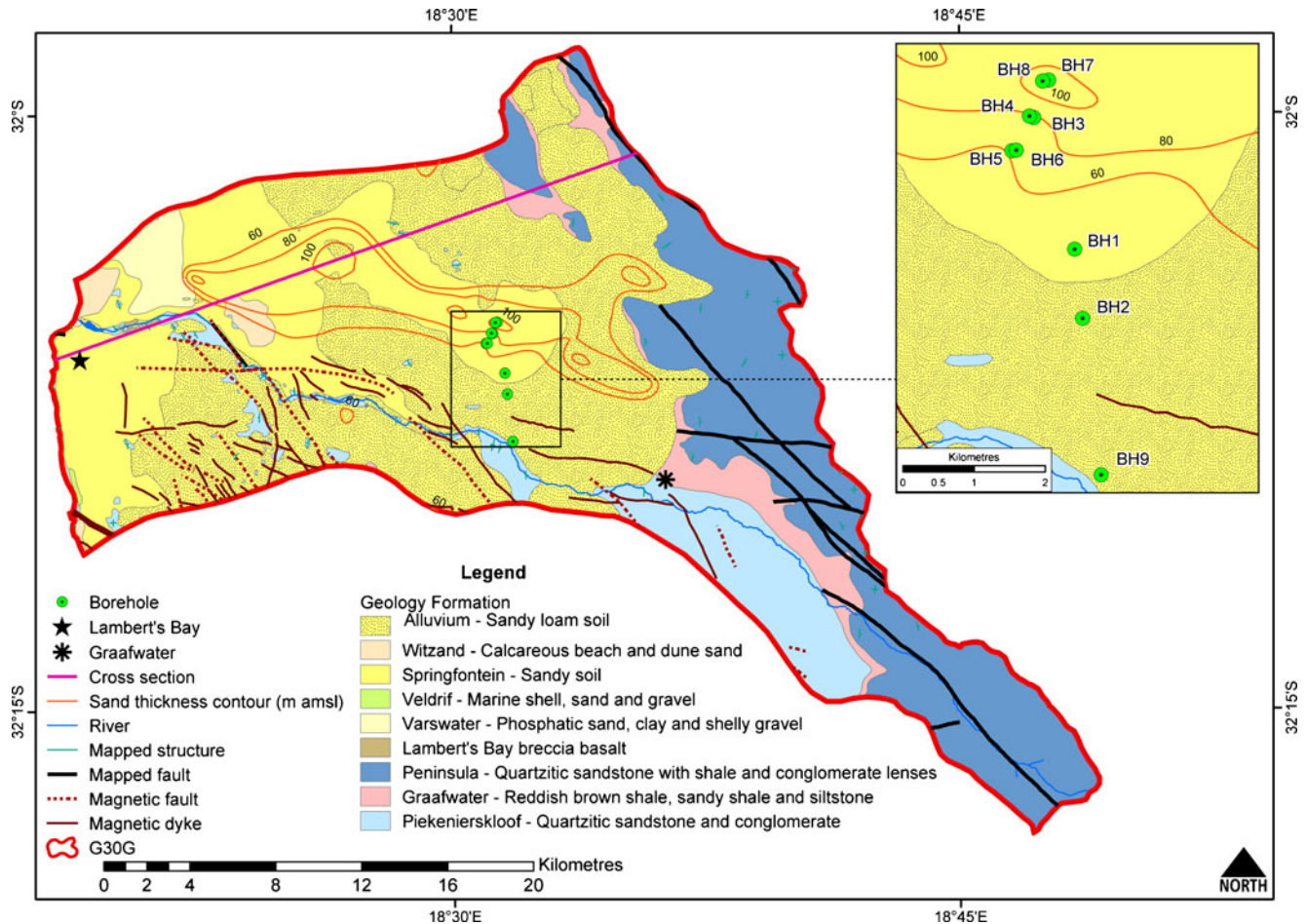
Fig. 4 Geology of G30G catchment (after de Beer 2003)

often covered by sand. In the sand covered areas, the differentiation between faults and inferred faults is based primarily on the presence or absence of outcrops. The basement of G30G comprises the oldest formation of the TMG, the Piekenierskloof Formation comprising quartzitic sandstone and conglomerate (de Beer 2003). The great thickness and brittle nature of the Piekenierskloof Formation results in fracturing and contains a high-yielding aquifer with high-quality water and low mineralisation. The Graafwater Formation, which occurs between the Piekenierskloof and Peninsula formations, is a poor aquifer and is even considered an aquitard in places (de Beer 2003). Borehole yields are typically low and the water quality is poor (GEOSS 2006). The Peninsula Formation is an extremely important hydrogeological unit and has proven to be a high-yielding aquifer in places. Its competent character and gritty, pebbly sandstones give it a favourable permeability and transmissivity. The water quality from the Peninsula Formation is typically very good with a low overall mineralisation and particularly low alkalinity (de Beer 2003).

The sandy Cenozoic cover is agriculturally the most intensively exploited succession in the Sandveld. Its high porosity and high horizontal permeability result in high borehole yields within this primary aquifer deposit. Interestingly, according to Nel (2005), the vertical recharge

reduces to almost zero in the western portion of the study area, yet the primary aquifer, Graafwater Primary Aquifer, indicated by the sand thickness contours (Fig. 4), is very high yielding in this area. This is attributed to the high groundwater flows within the fractured bedrock that result in recharge occurring upward from beneath the sands. The highest borehole yields occur where the primary aquifer is targeted above structurally favourable features in the bedrock. In general terms, the water quality deteriorates from the mountainous recharge areas in the east of the study area towards the low lying, low recharge coastal region (GEOSS 2006).

According to Healy (2010) methods of estimating groundwater recharge can broadly be categorized as methods using the water-budget, modelling or tracer techniques as well as physical methods involving saturated and unsaturated zones. Several approaches use precipitation to quantify groundwater recharge (Brunner et al. 2004) and most of these methods yield point values of recharge with large uncertainties (Healy 2010; Szilagyi et al. 2011). Many of these methods have been applied in the Sandveld, and point values for recharge, associated with boreholes in the study area, have been calculated (GEOSS 2003, 2006; Nel 2005). Some of the methods used in quantifying groundwater recharge in the Sandveld (Table 1) include the chloride mass

Table 1 Methods used to quantify groundwater recharge in the Sandveld and the estimated recharge values as percentage of rainfall

Method	Percentage (range)
Chloride mass balance (CMB)	
GEOSS 2006	1.2
Nel 2005	7–37[a]
Saturated volume flow (SVF)	
GEOSS 2006	1.7
Cumulative rainfall departure (CRD)	
GEOSS 2006	1.8
Nel 2005	0.2
EARTH	
GEOSS 2006	3.4
Conrad et al. 2004	0.2–3.4

[a] 37 % outside study area, but expected to contribute (Nel 2005); highest measured value 11 %

balance (CMB) method, cumulative rainfall departure (CRD) method, saturated volume flow (SVF) method and the Extended model for Aquifer Recharge and soil-moisture Transport through the unsaturated Hardrock (EARTH) method (Xu and Beekman 2003).

The application of point values does not cater for the spatial and temporal variability of recharge which is required to enable effective water-resource management at the regional level (Scanlon et al. 2002). Using a spatial model which included effective recharge as well as calculated inflow and outflow to the catchment based on elevation gradient at the catchment boundary, GEOSS (2006) estimated the total recharge for G30G at regional level as 6.8 % of rainfall. Following a water-balance approach, Timmerman (1986) suggested a conservative estimate of 8 % regional recharge for the Graafwater area based on previous work on the sandy aquifers of the West Coast region of South Africa (Bredenkamp and Vandoolaeghe 1982; A. Gerber, Water Research Commission, unpublished report, 1980; Timmerman 1985a, b; Vandoolaeghe and Bertam 1982) as reported by Jolly (1992).

Methodology

The research methodology is based on a simplified water balance where the difference between precipitation (P) and evapotranspiration (ET) is indicative of recharge or discharge over a period of time based on catchment average values (Brunner et al. 2004, 2007; Szilagyi et al. 2011, 2012) for a quaternary catchment. The standard water-balance equation is given as:

$$P + Q_{on} = ET + \Delta S + Q_{off} \qquad (1)$$

where P is precipitation, Q_{on} is run-on (surface and groundwater), ET is actual evapotranspiration, ΔS is change in storage (groundwater and soil water) and Q_{off} is run-off (surface and groundwater).

As suggested by Brunner et al. (2004, 2007), the potential recharge rate over long time intervals for flat terrain, can be

calculated from P and ET if steady-state conditions are assumed. This method is based on the concept of the zero-flux plane (a horizontal plane in the unsaturated zone). Above the zero-flux plane, water moves upwards in response to evapotranspiration and vertical movement downwards may contribute to recharge (Healy 2010). Using a simple water-balance equation, change in water storage at the zero-flux plane (ΔS^{uz} can therefore be defined as:

$$\Delta S^{uz} = P - ET - R_{off} \qquad (2)$$

In this study area, the surface runoff can be regarded as negligible as the Jakkals River is essentially non-perennial, as in the dry and hot summer months the river system stops flowing (GEOSS 2003; DWAF 2011). Thus, the standard water-balance equation for this semi-arid catchment can be simplified:

$$\Delta S^{uz} = P - ET \qquad (3)$$

where ΔS^{uz} therefore represents the potential contribution to groundwater recharge.

Based on this assumption, catchment P and ET from existing earth observation data products, calculated independently of each other for the period 2000–2011, are used to determine the groundwater recharge potential. Further to this, a new earth-observation evapotranspiration model, ET_{MODIS} (Palmer and Yunusa 2011), and the Pitman rainfall-runoff water-balance model (Hughes 2004), which is routinely implemented in South Africa, are applied and used for comparative purposes.

The monthly P and ET for all data products are separately summed to indicate the cumulative P and ET over the study period and the monthly and annual long-term (12 years) averages. The catchment water balance for the study period is presented for the MOD16 evapotranspiration product (Mu et al. 2011), ET_{MODIS} and Pitman models. Additionally, the within-catchment recharge and discharge zones are identified through spatial representation of the long-term results of the simplified water balance calculated using P (ARC-ISCW decadal grid) and the MOD16 data product.

Precipitation

The ARC-ISCW decadal rainfall grid is a data product created from downloaded satellite rainfall data from the African Data Dissemination Service and automatic weather station rainfall data (ARC-ISCW Ten Daily Rainfall Estimate Grids. Grid metadata, 2005), which are combined and interpolated to create a 1-km rainfall grid representing precipitation for a 10-day period across South Africa. Each grid identifies the decadal rainfall total in mm at a 1-km resolution, whereas the resolution of the original satellite rainfall estimate is 8 km. These data are summed to obtain the total monthly and annual rainfall over the study period, as

well as the 12-year average, allowing for regional modelling rather than analysis at microclimate scale (ARC-ISCW Ten Daily Rainfall Estimate Grids. Grid metadata, 2005).

Rainfall measurements from ARC-ISCW manual weather stations, in and around the G30G catchment (Fig. 5) not used in the creation of the data product, were used to validate the monthly and summed annual rainfall data. Monthly data for each manual weather station were compared to monthly gridded data extracted for the pixel at the weather-station location. Both gridded and weather station data per month were averaged over the study period and compared to analyse the temporal accuracy of the ARC-ISCW rainfall grids. The weather-station annual rainfall data were also compared to the annual pixel value. To assess the spatial accuracy of the 12-year average ARC-ISCW rainfall data, it was compared to the raster database of rainfall for Southern Africa (Lynch 2004), a 1-arc-minute precipitation grid generated from 9,600 weather stations with ≥15 years of daily records.

Evapotranspiration

The MOD16 ET products are regular 1-km^2 global land surface ET datasets for vegetated land areas at 8-day and monthly intervals (Mu et al. 2011). The ET products are created using MODIS global landcover (MOD12Q1), a daily meteorological reanalysis data set from NASA's Global Modelling and Assimilation Office, and MODIS biophysical parameters—albedo, Leaf Area Index (LAI) and Enhanced Vegetation Index (EVI)—as input into the Penman-Monteith equation. The MOD16 data product (mm per month; Mu et al. 2011) was downloaded from the Numerical Terradynamic Simulation Group website (NTSG 2000–2011) for the study period (2000–2011).

There is currently insufficient observed data in the study area to validate the MOD16 data product but validating MOD16 is recognised as a research priority in South Africa (L.A. Gibson, GEOSS, personal communication, 2012). Mu et al. (2011) undertook an extensive validation of the MOD16 data product and reported mean average errors of 0.33 mm/day (24.1 %); and correlation
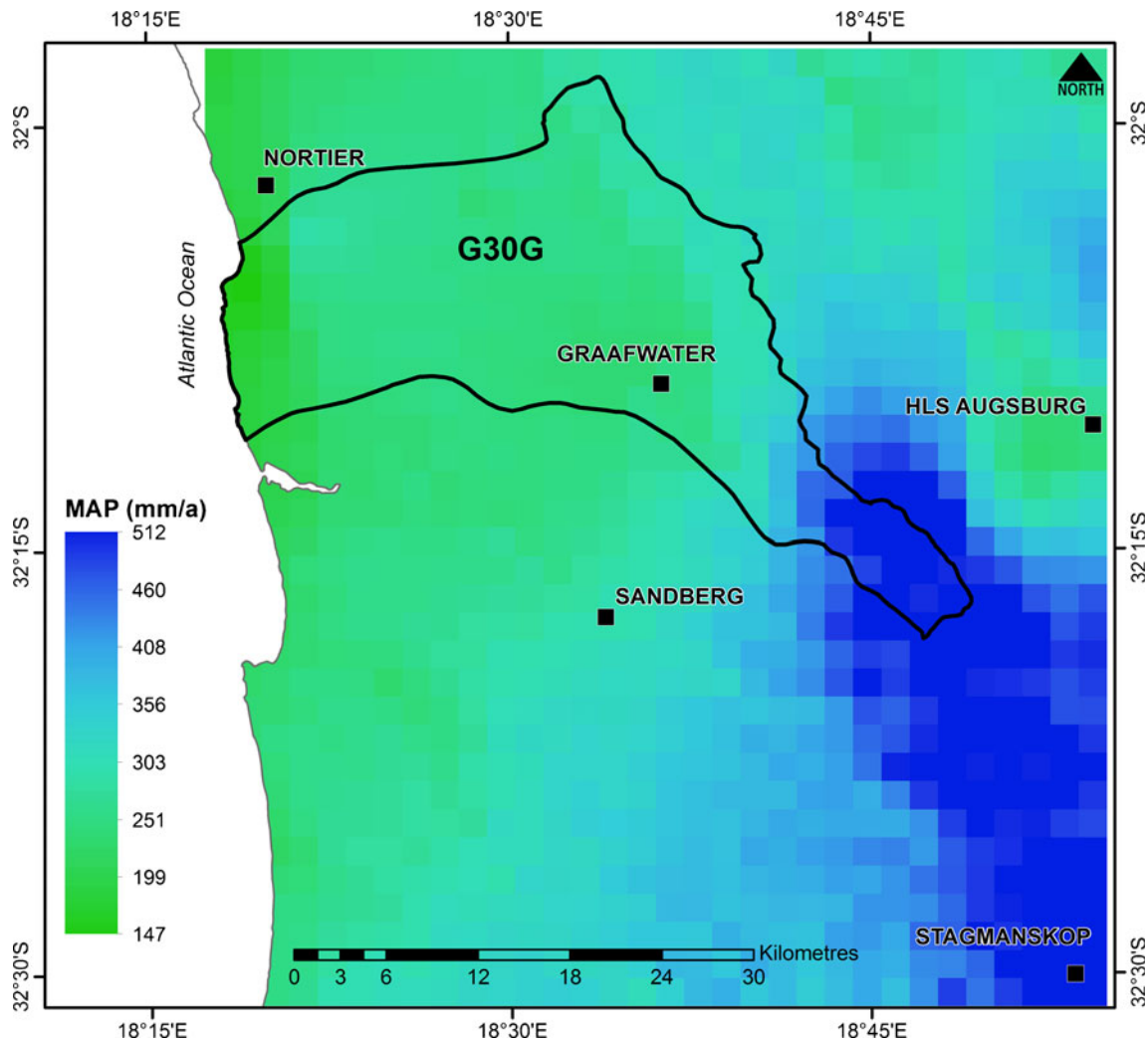

Fig. 5 Locations of manual weather stations used in the validation of the ARC-ISCW rainfall grid, with mean annual precipitation (*MAP*)

coefficients of 0.86, when compared with 46 AmeriFlux eddy covariance flux tower measurements across seven biomes. Mu et al. (2011) state that this is within the reported 10–30 % accuracy range to be expected from remote-sensing methods (Kalma et al. 2008).

Additionally, an alternative parsimonious earth observation evapotranspiration model, ET_{MODIS}, (Palmer and Weideman 2011; Palmer and Yunusa 2011) was applied to the study area. The model calculates ET by combining FAO56 and the MODIS LAI product (MOD15A), in a manner that approximates Mu et al. (2011) and follows on from earlier research (Cleugh et al. 2007; Leuning et al. 2008, 2009) to estimate actual ET using earth observation data. In ET_{MODIS}, the MODIS LAI product is used to approximate canopy conductance in the Penman-Monteith equation (FAO56) by invoking functional convergence theory (Field 1991). This alternative approach was applied to the catchment and is presented for comparative purposes. Pre-processed MODIS images (MOD15A, Collection 5) were acquired from the Land Processes Distributed Data Archive for the study period. Mean LAI values were extracted for the entire catchment for each 8-day period from November 2002 until December 2011. These mean LAI values are used to compute daily ET (mm) by adjusting the Penman-Monteith equation (FAO56; Allen et al. 1998) using the function:

$$ET_{MODIS} = \left(\frac{LAI}{LAI_{max}} \right) \times ET_0 \times k \qquad (4)$$

where LAI is the mean MODIS LAI for that 8-day period; LAI_{max} is the maximum retrieved at the site over the whole MODIS data record (~500 records); ET_0 is calculated from hourly meteorological data from an automatic weather station (Sandberg 32.29°S, 18.57°E) using FAO56; and k is an optimised scaling factor which relates leaf-level conductance to canopy conductance. This equation has been applied successfully to predict actual ET measured at another study site where the predictions were validated against an eddy covariance system (Palmer and Weideman 2011). In this study, the weather station was approximately 30 km away from the eddy covariance tower but did not appear to severely limit the ability to predict ET using the model, suggesting that in a small relatively homogeneous catchment, with moderate variation in elevation, it is permissible to use data from only one automatic weather station. Following Palmer and Weideman (2011), during the wet season (1 April—31 October), $k=1$, while during the dry season (1 January–31 March; 1 November–31 December), $k=0.65$.

The Pitman rainfall-runoff model

The Pitman monthly rainfall-runoff model (Hughes 2004; Hughes et al. 2006), developed for South African conditions, was applied to the study area as an alternative to validation via inter-model comparison. Conceptually, the study area was divided into two sub-catchments, one representing the headwater areas with steep topography and higher rainfall (226.5 km^2) and the other representing the lower-lying coastal areas with lower rainfall (420.9 km^2). Gridded rainfall data for the period October 2000 to September 2011 were used in the model run and a fixed seasonal distribution of potential evaporation based on observed A-pan evaporation data from the Graafwater weather station (20069). In setting up the model, it was assumed that the stream flow is derived largely from intermittent surface runoff and that baseflows do not form a significant component of the stream flow regime. Recharge in the headwater area was assumed to be high (mean annual value of approximately 70 mm/a) based on Nel (2005) and that a large proportion (simulated as 92 %) would be transferred to the lower-lying coastal areas in the sub-surface environment.

Results

Precipitation

The monthly variability of rainfall could affect the accuracy of the gridded product. The root mean square error (RMSE) and mean absolute error (MAE) of the monthly average gridded data as compared to the average weather station data per month are shown in Table 2. Largest variations between gridded and weather station data occur in the months May to July as illustrated in Fig. 6. The biggest errors occur at weather stations that lie outside the catchment of interest (Stagmanskop, Augsburg and Sandberg), while the gridded data at Graafwater (site code 20069; within catchment G30G) shows better agreement with measured rainfall data.

The correlation between measured rainfall per weather station per month as compared with the associated value extracted from the ARC-ISCW decadal grid at the particular weather station, is shown in Table 3 as well as the overall RMSE and MAE for the station.

There is a good correspondence between the ARC-ISCW rainfall grid and the rainfall recorded at the manual weather stations, with the RMSE varying between 6.46 mm at Nortier (MAE of 3.97 mm) on the coast (with the lowest measured annual rainfall of 224 mm average for the 12 year period) and 13.18 mm for Stagmanskop (MAE 7.59 mm) measuring 488 mm for the same period. Sandberg and Augsberg, situated further away from the coast but at low elevation, deviate further from the gridded results with a correlation of 0.84. Since RMSE is more sensitive to single large outlier values as found at Sandberg, the MAE for this weather station is a better indicator of accuracy (4.34 mm) than the RMSE of 11.17 mm.

The results of a spatial comparison of the 12-year average ARC-ISCW rainfall data set with the Lynch (2004) raster database (Gmap) are illustrated in Table 4, basic descriptive statistics per data set.

The ARC-ISCW grid has a cell size of 1 km, while Gmap has a resolution of 1 arc minute (~ 1.8 km). Since

Table 2 RMSE and MAE of monthly average gridded data compared to weather station data

Month	Graafwater 20069[a]		Nortier 20087		Stagmanskop 20127		HLS Augsburg 20145		Sandberg 30174	
	RMSE	MAE	RMSE	MAE	RMSE	MAE	RMSE	MAE	RMSE	MAE
Jan	3.31	1.81	5.47	2.64	3.62	2.02	3.05	2.23	3.89	2.25
Feb	3.72	1.88	4.77	2.94	4.77	2.96	4.72	2.42	3.28	2.33
Mar	1.96	1.27	2.20	1.52	3.04	1.93	5.92	3.86	4.88	2.45
Apr	6.99	4.59	3.33	2.55	11.51	7.61	4.77	3.88	11.96	8.02
May	9.96	6.22	7.62	5.01	15.72	12.05	15.32	9.38	29.90	12.28
Jun	8.49	6.12	9.97	7.62	24.17	15.18	10.42	8.37	4.99	2.90
Jul	15.68	9.32	10.08	6.44	19.90	12.64	13.54	7.73	12.53	6.70
Aug	12.07	8.77	7.34	5.27	14.31	9.88	15.19	10.48	3.03	1.82
Sep	5.06	3.63	5.39	3.66	14.97	9.18	9.24	5.67	1.88	1.20
Oct	3.18	2.17	8.07	5.46	10.60	7.07	5.22	3.43	7.86	4.40
Nov	6.27	4.83	4.16	2.59	8.49	5.42	4.96	3.10	10.30	5.18
Dec	9.21	5.47	2.76	1.87	7.84	5.15	5.17	2.68	4.65	1.75

[a] Number represents the site code for the weather station

Gmap uses slope as one of its input parameters (Lynch 2004), this combined with the coarser resolution may cause smoothing of extreme values, especially in mountainous areas. Figure 7 shows the standardized residual of spatial linear regression between the two data sets visualized with a hillshade data set to show relief as backdrop. Figure 7 indicates clearly the effect of topographically heterogeneous areas on the difference between the data sets. Despite the resolution difference, the mean rainfall differs by less than 10 % with a Pearson correlation of 0.82 on the same spatial extent; indicative of a statistical acceptable result.

Evapotranspiration

Actual evapotranspiration (ET_{MODIS}) for the G30G catchment was calculated and benchmarked against the MODIS ET data product (MOD16). At both a monthly and annual time scale, the ET_{MODIS} returns a lower ET than the MOD16 data product with a mean monthly ET of 15.9 mm for ET_{MODIS} and 19.3 mm for MOD16. The correlation between the two data sets on a monthly basis is only 0.234, implying that the use of a common variable (MODIS LAI) in the creation of each dataset does not create a correlation bias between the datasets. The results of accumulated monthly ET (mm) and rainfall data (mm) for each calendar year are shown in Fig. 8. The ET_{MODIS} is lower than MOD16 in all cases. This difference between ET_{MODIS} and MOD16 is more pronounced in wet years, with a difference of up to 30 %. The models tend to concur best in average years when rainfall does not appreciably exceed ET, with model results deviating further in wet years.

Validation data using field-based techniques for measuring evapotranspiration (e.g. eddy covariance or scintillometry) are currently unavailable for this catchment and this research caveat is acknowledged. The closest field-validation data publically available is from a field campaign conducted in November 2008 by Jarmain and
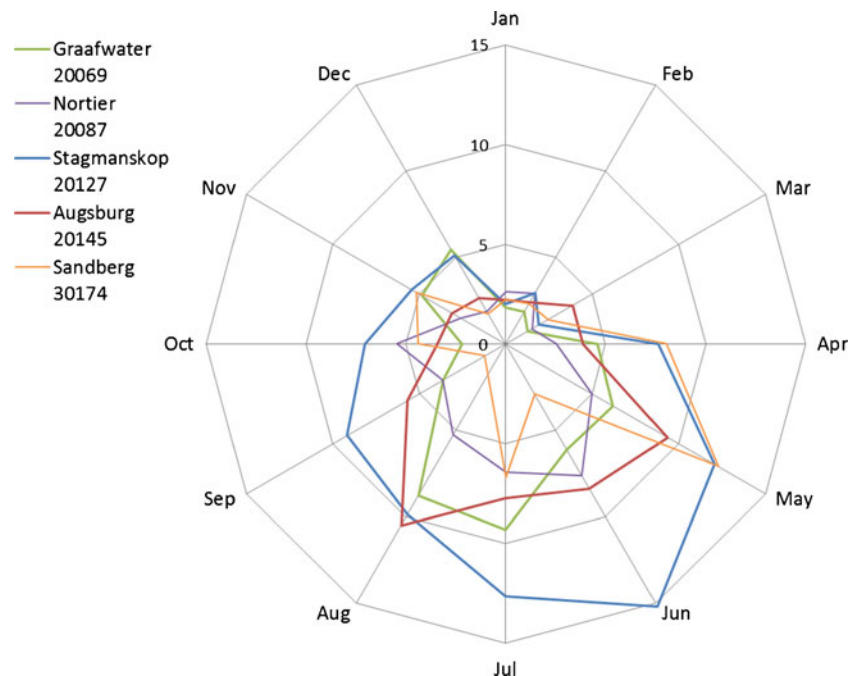

Fig. 6 Mean absolute error (MAE) for monthly average rainfall for validation weather stations

Table 3 Weather station elevation and 12-year average rainfall, r^2, *RMSE* and *MAE* values showing goodness of fit between weather station data and ARC-ISCW grid results for catchment G30G

	Graafwater 20069	Nortier 20087	Stagmanskop 20127	HLS Augsburg 20145	Sandberg 30174
Elevation (m amsl)	205	98	597	89	93
Average P (mm)	287	224	488	233	292
r^2	0.91	0.92	0.93	0.84	0.84
RMSE	8.19	6.46	13.18	9.18	11.17
MAE	4.69	3.97	7.59	5.27	4.34

Mengistu (2009) using an eddy covariance system in catchment G10K ~70 km to the south of the study area. The daily average field-validation data (4.7 mm/day) for November 2008 is compared with daily average MOD16 ET data product (2.71 mm/day) for the corresponding MODIS pixel. Although this implies an underestimation of 2 mm/day (42 %) by MOD16, it should be noted that the MOD16 is representing a mixed landcover including natural vegetation, whereas the field campaign was conducted in a large (3.18 ha) irrigated apple orchard. Therefore, the MOD16 ET result cannot accurately be validated using only this dataset; however, the low estimate is noted and provides motivation for the urgent local validation of MOD16.

ET as modelled by ET_{MODIS} shows a larger monthly variation (var=28.43) than MOD16 (var=19.35). This difference in variance was significant when measured with the Fischer F-test. A lower annual trough occurring in May is apparent for ET_{MODIS}. There seems to be an interesting similarity in the synchronicity of the peaks and troughs (Fig. 9) in the MOD16 product and ET_{MODIS}; however, the quantum of the peaks does not concur. Both models establish that although there is a high evaporative demand in the summer months (confirmed by high ET_0), the evapotranspiration is limited by the availability of water. The lower variance in the MOD16 results is considered a remnant of the global meteorological surfaces used in the creation of the MOD16 data product implying that the ET_{MODIS} results may be locally relevant whereas the MOD16 results may be regionally relevant.

The Pitman rainfall-runoff model

For some local measure of the accuracy of ET estimates, MOD16 ET values were compared to the output from the Pitman monthly rainfall-runoff model (Hughes 2004; Hughes et al. 2006)(Fig. 9). The Pitman model predicted a monthly average total ET of 20.1 mm for the headwater catchment and 24.7 mm for the downstream catchment. The downstream ET was dominated by losses from rainfall contributing to soil-moisture storage (87 %), with

Table 4 Descriptive statistics comparing ARC-ISCW rainfall grid with Gmap (mm; after Lynch 2004). *SD* standard deviation

	ARC-ISCW grid	Gmap
Mean	309	283
Min	167	147
Max	679	512
SD	79	69

smaller contributions from groundwater losses (11 %) and irrigation water (2 %). The pattern of variation of downstream ET is very dependent upon the maximum soil-moisture-storage-parameter value and converges on the ET_{MODIS} pattern of variations as this parameter is increased from about 200 mm to 1,000 mm, a result that is consistent with the deep sands found in this area. The simulated water-balance components are given in Table 5 and while there are a number of uncertainties associated with the way in which the model and the parameter values are used to represent the catchment's hydrological response, the results are consistent with what is reported in the literature about the hydrology of this region (GEOSS 2006; Jolly 1992; Nel 2005; Timmerman 1986). It should however be noted that in the model, the groundwater inflow to the downstream catchment does not interact directly with the overlying soil-moisture storage. This model limitation will affect the total evapotranspiration in the downstream catchment by limiting the amount of water available to evaporate.

Groundwater

Monthly groundwater levels in selected boreholes in G30G for the study period (locations indicated in Fig. 4) are plotted together with the catchment average rainfall (Fig. 10). These are monitoring boreholes; thus, abstraction from nearby boreholes may contribute to water-level fluctuations. Boreholes 1, 3, 5 and 6, of similar depth in the sandy soil, have the same water-level trend and have been combined for ease of interpretation. Boreholes 4 and 8, in the sandy soil, have deeper water levels but also a similar water-level trend. Borehole 9 shows the greatest water-level fluctuation when compared to rainfall variation. Abstraction for irrigation from boreholes also targeting the high-yielding Piekenierskloof Formation (of which there are at least six within a 1 km radius) will have an impact on the water level in this borehole.

Water balance

In Fig. 9, the long-term monthly average results of P, ET_{MODIS}, MOD16 and simulated Pitman are plotted and in Fig. 11 the cumulative ET and P results, as well as P–ET (MOD16) are plotted. The typical rainfall pattern of the study area is apparent with very little rain falling in the hot summer months and consistent rain falling in the winter months with the highest rainfall occurring in July. When considering only vertical recharge, Figs. 9 and 11
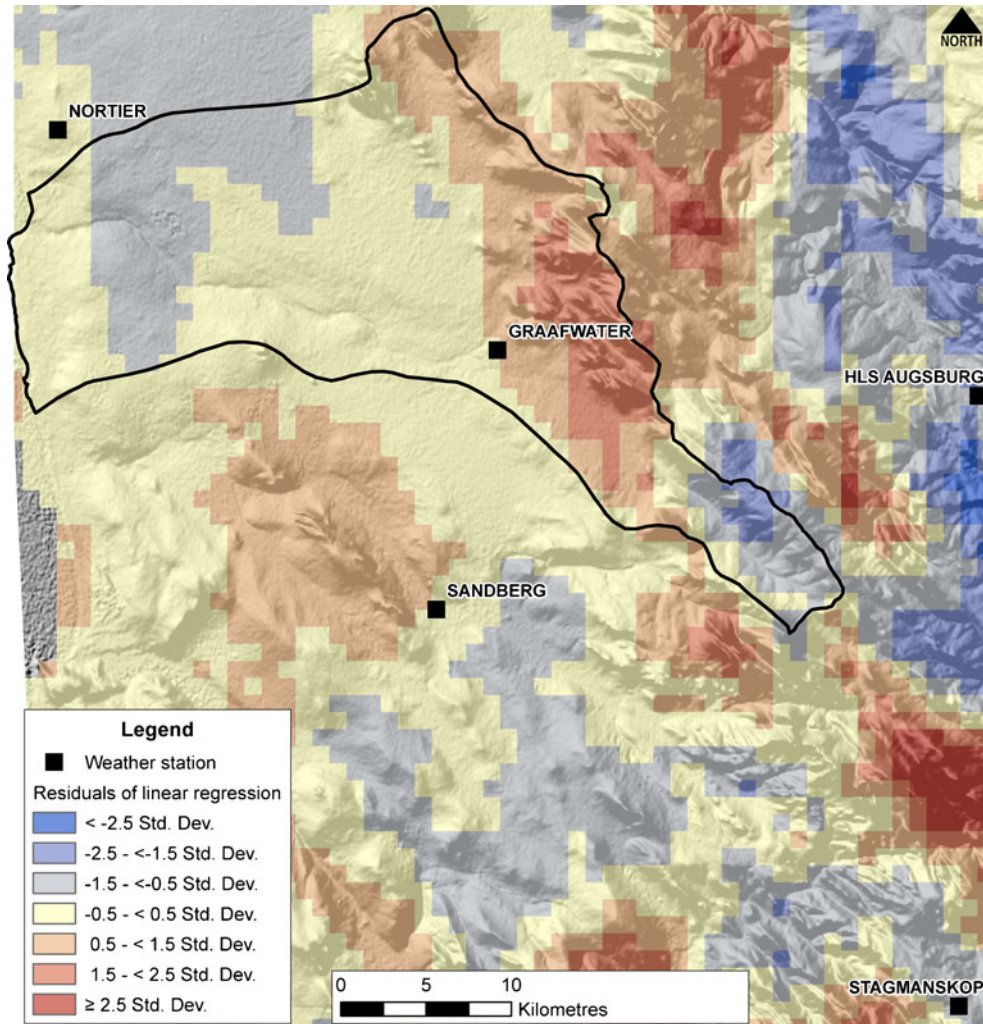
Fig. 7 Residuals of linear regression between ARC-ISCW rainfall product and Gmap raster rainfall database (after Lynch 2004) with a hillshade as backdrop

demonstrate that ET is not supported by precipitation alone in the hot summer months (November to May). Even though the Pitman model results are very similar to the recharge results derived from remote sensing, initial

fixed model soil-moisture storage plays an important role in achieving these results (Table 5). In addition, since the Pitman model does not have the mechanism accounting for lateral flow of groundwater in a confined system,
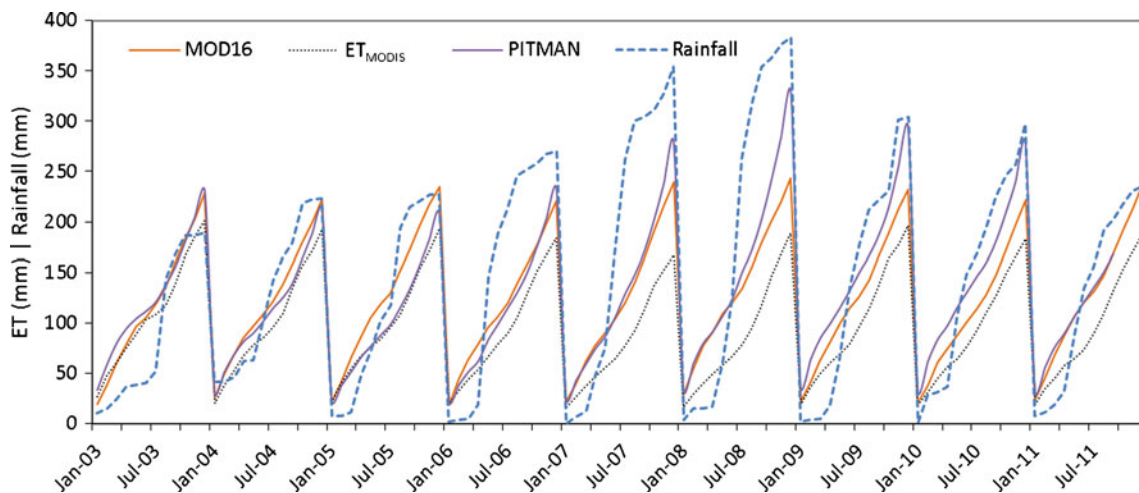

Fig. 8 Annual comparison of rainfall, MOD16, ET_{MODIS} and Pitman model patterns for the study period
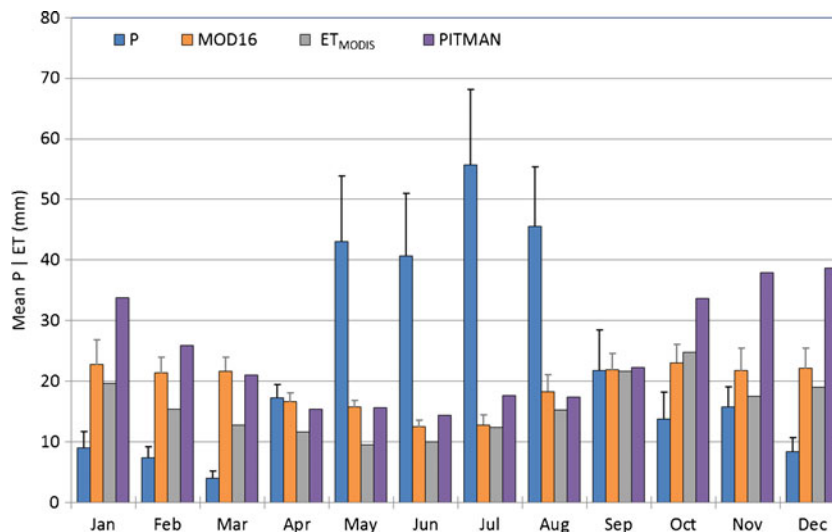
Fig. 9 Monthly catchment average MOD16 and ET$_{MODIS}$ values compared to Pitman model ET output and catchment average rainfall from ARC-ISCW

the 20 % groundwater outflow from the headwater catchment subsequently entering the downstream catchment may in reality interact with overlying soil-moisture storage within the zone at and above the water table. Where the groundwater levels are shallow in the downstream catchment the high capacity of the soil-moisture storage will contribute to higher ET than precipitation. Lateral regional groundwater flow plays a role in supplying the downstream catchment with groundwater via hydraulically connected geological structures. The presence of outcrops of bedrock in the sand in the lower catchment may be indicative of alternative preferential flow pathways, but is not proven by this particular result.

As seen in Fig. 10, borehole 9, located in the Piekenierskloof Formation, consistently shows a drop in water level in response to the dry summer conditions but

recovery associated with rainfall is rapid due to direct (vertical) recharge to the unconfined aquifer. Borehole 8 shows a similar seasonal trend. In contrast, the groundwater levels in boreholes 1–6, which are all found in the sandy Cenozoic cover of the Graafwater Primary Aquifer, remain constant throughout the study period, fluctuating by less than 0.5 m even during the dry summer months. Recovery of water levels after rainfall events is not evident for these boreholes implying that direct recharge does not occur in these areas. From drilling in this area, it has been noted that a clay layer is often found beneath the sand acting as a confining layer. Recharge of a confined aquifer is often indirect from beneath, or lateral, which may explain the low range of variation for many of the boreholes, and a delayed response of recharge from rainfall.

Variation in the cumulative monthly P, ET and P–ET (ET=MOD16) over the study period is provided in Fig. 11.

Table 5 Water-balance components in mm average per month (sub-components are indented)

Components and sub-components	Headwater catchment (226.5 km^2)		Downstream catchment (420.9 km^2)	
	Component	Sub-component	Component	Sub-component
Rainfall	26.00		19.33	
Incremental runoff	0.82		0.03	
Upstream inflow	0.00		0.44	
Channel losses		0.00		0.27
Downstream flow		0.82		0.20
GW recharge	5.56		0.16	
GW inflow	0.00		2.75	
GW from channel	0.00		0.27	
GW outflow		5.12		0.03
GW evaporation		0.44		2.80
GW abstraction		0.00		0.36
Total evaporation	20.06		24.73	
From soil		19.62		21.57
From GW		0.44		2.80
From irrigation		0.00		0.36
Changes in storage	0.00		−2.43[a]	

GW groundwater

[a] Large negative change in storage is a reflection of the high starting soil-moisture level (fixed in the model) which is not even achieved during wet years in the simulation
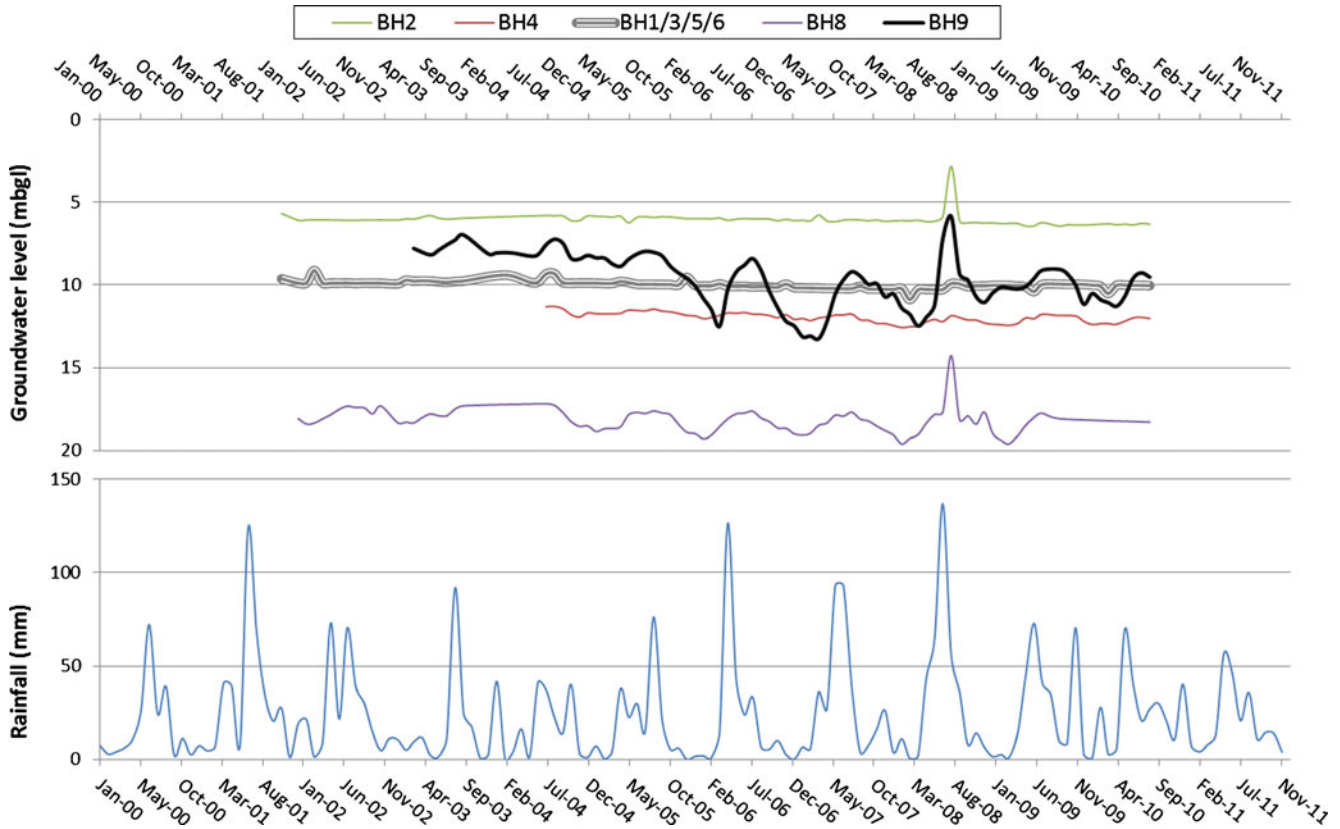
Fig. 10 Groundwater levels (m below ground level) in G30G and ARC-ISCW catchment average rainfall over time

At the catchment scale ET reaches a maximum in December, however, the minimum P–ET is reached in March. Precipitation in the months May to August allow the long-term P–ET budget to close on a positive value with a catchment average value for P at 282±65 mm/a and total ET (MOD16) of 231±28 mm/a, leaving an excess of 51±80 mm/a or 13±25 %. The catchment average is higher than the recharge percentage from various

traditional methods or values reported in literature (0.2–8 %). Higher recharge values would be expected if ET is underestimated using the MOD16 data products. However, Nel (2005) reported 20–100 mm/a (up to 37 % recharge) in the mountainous parts of G30G and adjacent catchment associated with higher rainfall and isotope results confirm the higher recharge to these areas (GEOSS 2006).
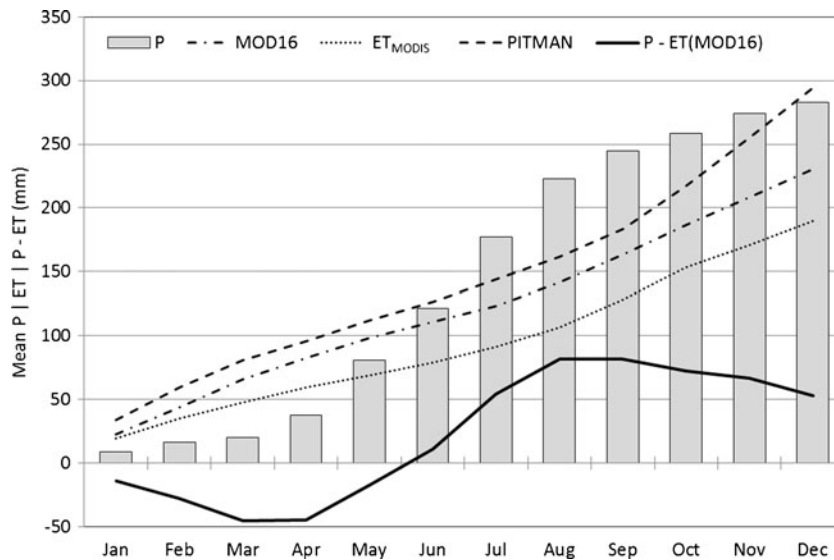

Fig. 11 G30G water balance showing cumulative monthly values from ARC-ISCW *rainfall* grids, ET_{MODIS} and *Pitman* models and *MOD16* data product

Figure 12a shows the spatial distribution of recharge zones as defined by long-term (P–ET)/P. The highest recharge occurs at higher elevation associated with higher rainfall, as well as sandstone of the Peninsula Formation. The areas marked "No data" in Fig. 12a and b are created from the MODIS data product which identified the particular cell as non-vegetated. Available groundwater chloride values for G30G are shown in Fig. 12b. Recharge ratios calculated using the CMB method (Conrad et al. 2004; GEOSS 2006) for boreholes with a groundwater chloride value less than 1,000 mg/L are illustrated. Boreholes penetrating the Graafwater Formation have poor water quality with electrical conductivity up to 400 mS/m (Jolly 1992) and were not used in the CMB method.

Of particular interest is the area west of the deep sand indicated in Fig. 4 by the sand thickness contours, labelled "Inferred fault" in Fig. 12b. Indicative of an underlying fault system (paleochannel) not mapped, this area was targeted by GEOSS in 2007 for exploration purposes leading to a successful borehole with yield of ~11 L/s at a depth of 115 m. Recharge is anticipated to occur from the underlying fault at the contact zone between the formations.

There is considerable uncertainty in an assessment of this nature with remote-sensing products reported to have an error of 10–30 % (Kalma et al. 2008; Glenn et al. 2010). There is uncertainty associated with both the rainfall and ET data products, which is compounded when integrating these data into water-balance calculations. ET is a component of particular uncertainty in this study since it has not been validated in the field. Overestimation by MOD16 of ET by 10–30 % would increase the catchment average potential recharge from 13±25 % to between 22±22 and 39±18 %. However, if MOD16 underestimates ET by the reported 10–30 %, the catchment average potential recharge would decrease from 13±25 % to between 4±27 and −13±32 %, which would mean that this catchment is extremely sensitive and additional water allocation needs to be carefully considered. In Fig. 12b, where the ET has been corrected for underestimation of 20 %, the irrigation areas in the lower catchment where ET is greater than rainfall as a long-term average are obvious. The available recharge points were compared to the recharge potential output calculated using the different ET over- and underestimation scenarios. The best comparison with the CMB recharge values were found in the case of ET underestimation by 20 %. The RMSE for this scenario using 19 CMB recharge values was 19.6 % with a MAE of 19.1 %. The catchment average potential recharge in the case of 20 % underestimation of ET (Fig. 12b) would be −4±30 %. The high RMSE obtained when comparing point values to aerial values is indicative of the spatial variability of recharge (Cook et al. 1989) as well as the need for more recharge values for comparison with MODIS resolution data.

Discussion

Given the difficulties in obtaining accurate groundwater recharge estimates (Xu and Beekman 2003), especially at regional scale, using a simplified water balance approach can provide an approximation of recharge in a semi-arid environment. Since the modelled P appears accurate from the correlation with weather station data, actual spatial recharge can be calculated and calibrated using field data as suggested by Brunner et al. (2004, 2007). However, since ET validation data in this area are not available yet, and it is possible that the ET may be underestimated as reported by Mu et al. (2011) for crops, grass and closed shrubland, it is possible that overestimation of recharge can be expected from this method, which may lead to over-allocation of scarce resources.

The 9 years of data for ET_{MODIS} give about a 50/50 split between wet and average years. Functional convergence theory suggests that a natural ecosystem will optimise ecosystem efficiency by using most of the expected (~average) rainfall for ET, and indeed it is in average years when the models concur the best. Based on this theory, ET_{MODIS} appear to underestimate ET during wet years, with much lower annual ET estimates than even in the drier years. This is not a good result given that there is clearly more water available. MOD16 seems to perform more realistically under high-rainfall circumstances. The use of P–ET clearly identifies potential recharge and discharge zones, particularly in the absence of notable surface water interaction in this catchment. According to Nel (2005), there is no indication that any runoff occurs in the sand-covered areas of the Sandveld, except for runoff from hard road surfaces. The topographically lower area, which in the past experienced marine inundation with high-salinity levels, is clearly indicated as an area with negligible recharge not only due to low rainfall, but also high soil temperature and thick unsaturated sands with high soils chloride levels extending to 2 m below surface (Nel 2005). Local recharge through preferential flow paths can occur. The response of water levels in borehole 9, located in the thick, brittle Piekenierskloof Formation indicates that water-level drops due to dry summer conditions followed by rapid recovery associated with rainfall due to direct (vertical) recharge to the unconfined aquifer. The P–ET result demonstrates a recharge of 18±16 % at this borehole which could not be confirmed with the CMB method, due to the poor water quality of boreholes intersecting the Graafwater Formation (Jolly 1992). Studies in the arid central and southern Kalahari suggest recharge occurs only during periods of above-average rainfall along preferential lines, as in the vicinity of rock outcrops (Thomas and Shaw 1991) and zones of high infiltration (i.e. joints, zones of bioturbation, calcrete outcrops and drainage lines) (Mazor 1982). Groundwater levels in the thick sand remain constant throughout the entire season with delayed response to rainfall (boreholes 1–6 in Fig. 10). This is in keeping with findings by Van Straten (1955) who suggested that rainwater recharge would only
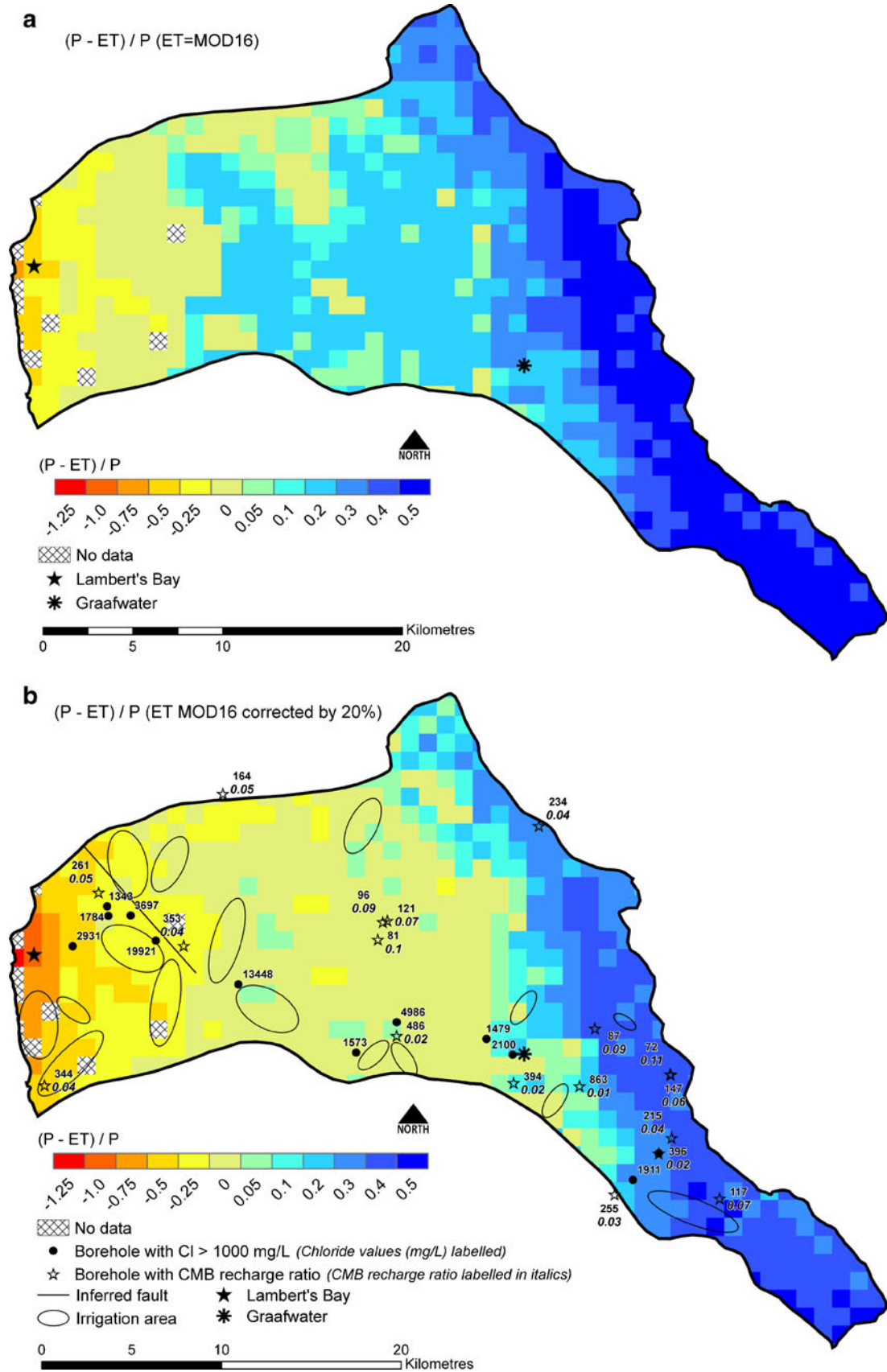
Fig. 12 Spatial distribution of recharge zones using **a** *P*–ET)/*P* with MOD16 data and **b** (*P*–ET)/*P* with ET corrected for 20 % underestimation, available groundwater chloride values (mg/L) and associated CMB recharge ratios

occur to a depth of 6 m, while Smit (1977) showed that recharge could be expected for unsaturated sand thickness less than 15 m for rainfall of 150 mm. Recharge of a confined aquifer, due to a clay layer below the sand, is often indirect from beneath or laterally.

Further, the benefits of applying the Pitman rainfall-runoff model to the catchment have been twofold. Firstly, the results have served to confirm that, for the catchment as a whole, the water balance resulting from the satellite data products is returning results which, although unvalidated, fall within the bounds of acceptable uncertainty for remote-sensing products (particularly ET). Secondly, it has been shown that the use of hydrological models can be more restrictive through strict parameter setting than when using a method such as proposed here, where each variable is calculated independently of the other. Thus, there is no constraint as to the outcomes of the water balance result.

The usefulness of identifying recharge zones is particularly demonstrated in the value added to conceptualizing the hydrogeology of the study area. The outcome of recharge calculations using the CMB method will always provide a positive value. The P–ET result indicates areas of "negative" recharge where discharge or inflow may be occurring. Figure 13 shows the west–east cross section indicated in Fig. 4 through the catchment identifying the different geological formations along the cross section.

The highest recharge from rainfall is associated with the high-lying eastern catchment boundary where high rainfall occurs and vertical recharge occurs into the sandstone of the permeable Peninsula Formation. Groundwater flows are generally from east to west through the fractured Piekenierskloof Formation which underlies the whole catchment allowing for fault-oriented flow in a SE–NW direction (identifiable by higher recharge in Fig. 12a). Lateral groundwater flow in the sand is minimal. Recharge to the sands occurs predominantly through preferential pathways associated with outcropping and faults as well as vertical leakage from the underlying bedrock. Recharge zones highlighted by the P–ET model coincide with mapped faults, as well as inferred faults not yet mapped. The low-lying area along the coast shows negative or no potential recharge in Fig. 12, yet from Fig. 3 it can be seen that agriculture is

practised. The chloride profile (Nel 2005) in these areas indicates that rainfall only saturates and flushes the top 2 m of the sand profile and that limited infiltration of high salt content can be expected, confirming minimal recharge of groundwater in these sand covered areas. The water to sustain this agriculture must therefore either be imported from the adjacent catchment to the south or pumped from boreholes within the recharge zone.

Conclusions and recommendations

From the conceptual model it seems that the main sources of water to the study area are faults (mapped and inferred) and rainfall recharge confined to the upper reaches of the catchment, reported in literature (GEOSS 2006; Jolly 1992; Nel 2005; Timmerman 1986) and supported by the P–ET model. The main occurrences of groundwater in the study area are associated with faults and the thick primary sand aquifers that are recharged from below. These primary aquifers support the agriculture and towns, as well as seasonal river ecology. The P–ET model assists in the conceptualization of the hydrogeological fluxes that occur specifically in areas of thick sand where faults and outcrops remain unmapped and recharge may be from below. In addition, the recharge calculated by the P–ET model is not unreasonable, especially when considering the potential underestimation of ET. However, if the ET is underestimated by more than 20 %, it would indicate that the catchment is under severe water stress. This study confirms that recharge will occur in the high-lying areas, especially during wet years, but that when the water availability trajectory is downwards, current agricultural practices will have to be reduced as the trend in the area already indicates. The results shown in Fig. 12, highlighting recharge zones, allow for better management of the scarce resource, since areas of water availability are highlighted.

It is recommended that the ET data products (MOD16) be validated in order to expand this P–ET model to the entire Sandveld, especially to catchments reportedly under severe stress such as G30F to the south. Within the stated caveats,
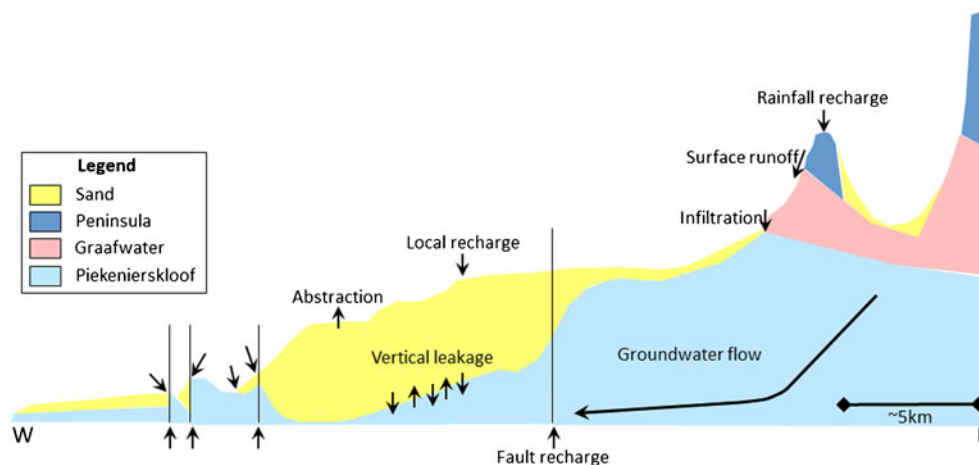

Fig. 13 Conceptual hydrogeology demonstrated by cross section of the catchment

the model can already be used to conceptualize the hydrogeology of the entire Sandveld, since it deals not only with direct downward vertical recharge but accounts for lateral recharge and recharge via the fault zones from below whilst indicating water use through evapotranspiration.

References

Ahmad M, Bastiaanssen WGM, Feddes RA (2005) A new technique to estimate net groundwater use across large irrigated areas by combining remote sensing and water balance approaches, Rechna Doab, Pakistan. Hydrogeol J 13:653–664

Allen RG, Pereira LS, Raes D, Smith M (1998) Crop evapotranspiration: guidelines for computing crop water requirements. FAO-Food and Agriculture Organization of the United Nations, Rome

Allen RG, Tasumi M, Morse A (2005) Satellite-based evapotranspiration by METRIC and LANDSAT for western states water management. Presented at the US Bureau of Reclamation Evapotranspiration Workshop, Feb 8–10, 2005, Ft. Collins, CO. Available online at http://www.idwr.idaho.gov/GeographicInfo/METRIC/PDFs/allen_et_al_metric_summary_paper2.pdf. Accessed 24 April 2013

Bastiaanssen WGM, Hellegers PJGJ (2007) Satellite measurements to assess and charge for groundwater abstraction. In: Dinar A, Abdel-Dayem S, Agwe J (eds) The role of technology and institutions in the cost recovery in irrigation and drainage projects, Agriculture and Rural Development Discussion Paper 33. The World Bank, Agriculture and Rural Development Group, Washington, DC, pp 38–59

Bredenkamp DB, Vandoolaeghe MAC (1982) Die Ontginbare Grondwater Potensiaal van die Atlantis Gebied [The exploitable groundwater potential of the Atlantis Area]. Department of Water Affairs, Cape Town, Report no. GH3227. Available online at http://www.dwa.gov.za/ghreport/. Accessed 24 April 2013

Brunner P, Bauer P, Eugster M, Kinzelbach W (2004) Using remote sensing to regionalize local precipitation recharge rates obtained from the chloride method. J Hydrol 294:241–250

Brunner P, Hendricks-Franssen HJ, Kgotlhang L, Bauer-Gottwein P, Kinzelbach W (2007) How can remote sensing contribute in groundwater modeling? Hydrogeol J 15(1):5–18

CapeNature (2006) Groundwater assessment of the north-west Sandveld and Saldanha Peninsula as an integral component of the Cape Fine-Scale Biodiversity Planning project. Component 5.1, Fine-scale biodiversity planning. Consultancy report submitted by GEOSS to CapeNature, Cape Town. Available online at http://bgis.sanbi.org/fsp/Reports/SandveldGroundwater.pdf. Accessed 24 April 2013

Cleugh HA, Leuning R, Mu Q, Running SW (2007) Regional evaporation estimates from flux tower and MODIS satellite data. Remote Sens Environ 106:285–304

Conrad J, Nel J, Wentzel J (2004) The challenges and implications of assessing groundwater recharge: a case study: northern Sandveld, Western Cape, South Africa. Water SA 30:75–81. Available online at http://www.ajol.info/index.php/wsa/article/viewFile/5171/12711. Accessed 24 April 2013

Cook PG, Walker GR, Jolly ID (1989) Spatial variability of groundwater recharge in a semiarid region. J Hydrol 111:195–212

Crosbie RS, Jolly ID, Leaney FW, Petheram C (2010a) Can the dataset of field based recharge estimates in Australia be used to predict recharge in data-poor areas? Hydrol Earth System Sci 14:2023–2038. doi:10.5194/hess-14-2023-2010

Crosbie RS, McCallum JL, Walker GR, Chiew FHS (2010b) Modelling climate-change impacts on groundwater recharge in the Murray-Darling Basin, Australia. Hydrogeol J 18(7):1639–1656

De Beer C (2003) The geology of the Sandveld area between Lambert's Bay and Piketberg (project 5510). CGS report no. 2003–0032. Council for Geoscience, Western Cape Unit, Bellville, South Africa

DWAF (2011) Classification of significant water resources in the Olifants–Doorn WMA. Inception report no. RDM/WMA17/00/CON/CLA/0111. Department of Water Affairs, Pretoria, South Africa. Available online at http://www.dwaf.gov.za/rdm/WRCS/doc/ODInceptionReportFinal25May2011.pdf. Accessed 24 April 2013

Field CB (1991) Ecological scaling of carbon gain to stress and resource availability. In: Mooney H, Winner S, Pell E (eds) Integrated responses of plants to stress. Academic, San Diego, pp 35–65

GEOSS (2003) Sandveld preliminary (rapid) reserve determinations. Langvlei, Jakkals and Velorenvlei Rivers, Olifants-Doorn WMA, vol 1, reserve specifications. DWAF project no. 2002–227. GEOSS, Stellenbosch, South Africa

GEOSS (2006) Groundwater reserve determination required for the Sandveld, Olifants Doorn Water Management Area, Western Cape, South Africa. Prepared for the Department of Water Affairs, Pretoria by GEOSS, Stellenbosch, South Africa

Gibson LA, Münch Z, Engelbrecht J (2011a) Particular uncertainties encountered in using a pre-packaged SEBS model to derive evapotranspiration in a heterogeneous study area in South Africa. Hydrol Earth Syst Sci 15:295–310

Gibson LA, Münch Z, Carstens M, Conrad JE (2011b) Remote sensing evapotranspiration (SEBS) evaluation using water balance. WRC consultancy report K8/929/1. Water Research Commission, Pretoria. Available online at http://www.wrc.org.za/Pages/DisplayItem.aspx?ItemID=9227. Accessed 24 April 2013

Glenn EP, Nagler PL, Huete AR (2010) Vegetation Index methods for estimating evapotranspiration by remote sensing. Surv Geophys 31:531–555

Glenn EP, Doody TM, Guerschman JP, Huete AR, King EA, McVicar TR, Van Dijk AIJM, Van Niel TG, Yebra M, Zhang Y (2011) Actual evapotranspiration estimation by ground and remote sensing methods: the Australian experience. Hydrol Process 25:4103–4116

Healy RW (2010) Estimating groundwater recharge. Cambridge University Press, Cambridge

Hendricks-Franssen HJ, Brunner P, Makobo P, Kinzelbach W (2008) Equally likely inverse solutions to a groundwater flow problem including pattern information from remote sensing images. Water Resour Res 44:W01419. doi:10.1029/2007WR006097

Hoffmann J (2005) The future of satellite remote sensing in hydrogeology. Hydrogeol J 13:247–250

Hughes DA (2004) Incorporating ground water recharge and discharge functions into an existing monthly rainfall-runoff model. Hydrol Sci J 49(2):297–311

Hughes DA, Andersson L, Wilk J, Savenije HHG (2006) Regional calibration of the Pitman model for the Okavango River. J Hydrol 331:30–42

Jarmain C, Mengistu MG (2009) Validating energy fluxes estimated using the surface energy balance system (SEBS) model for a small catchment. Consultancy report no. K8/824, Water Research Commission, Pretoria, South Africa

Jolly JL (1992) Geohydrology of the Graafwater Government Subterranean Water Control Area. Report no. GH3778, Dept. of Water Affairs, Cape Town, South Africa. Available online at http://www.dwa.gov.za/ghreport/. Accessed 24 April 2013

Kalma JD, McVicar TR, McCabe MF (2008) Estimating land surface evaporation: a review of methods using remotely sensed surface temperature data. Surv Geophys 29:421–469

Klock H, Udluft P (2002) Mapping groundwater recharge and discharge zones in the Kalahari: a remote sensing approach. In: Using geospatial technologies to understand dryland dynamics. Arid Lands Newsletter no. 51, May/June 2002. Available online at http://ag.arizona.edu/oals/ALN/aln51/klock.html. Accessed 24 April 2013

Leuning R, Zhang YQ, Rajaud A, Cleugh H, Tu K (2008) A simple surface conductance model to estimate regional evaporation using MODIS leaf area index and the Penman-Monteith equation. Water Resour Res 44:W10419. doi:10.1029/2007WR006562

Leuning R, Zhang YQ, Rajaud A, Cleugh H, Tu K (2009) Correction to "A simple surface conductance model to estimate regional evaporation using MODIS leaf area index and the Penman-Monteith equation". Water Resour Res 45:W01701. doi:10.1029/2008WR007631

Lynch SD (2004) Development of a raster database of annual, monthly and daily rainfall for Southern Africa. WRC report 1156/1/04. Water Research Commission, Pretoria, South Africa

Mazor E (1982) Rain recharge in the Kalahari: a note on some approaches to the problem. J Hydrol 55:137–144

Middleton BJ, Bailey AK (2008) Water resources of South Africa, 2005 STUDY (WR2005). WRC Contract K5/1491, Water Research Commission, Pretoria, South Africa

Midgley DC, Pitman, WV, Middleton, BJ (1994) Surface water resources of South Africa 1990, vols I–VI. Water Research Commission reports no. 298/1.1/94 to 298/6.1/94, Pretoria, South Africa

Mu QZ, Zhao MS, Running SW (2011) Improvements to a MODIS global terrestrial evapotranspiration algorithm. Remote Sens Environ 115:1781–1800. doi:10.1016/j.rse.2011.02.019

Mucina L, Rutherford MC (eds) (2006) The vegetation of South Africa, Lesotho and Swaziland. Strelitzia 19. South African National Biodiversity Institute, Pretoria, South Africa

Nel J (2005) Assessment of the geohydrology of the Langvlei Catchment. DWAF Report no. GH4000, Directorate: Hydrological Services; Sub-directorate: Groundwater Resource Assessment and Monitoring. Available online at http://www.dwa.gov.za/ghreport/. Accessed 24 April 2013

NTSG (Numerical Terradynamic Simulation Group) (2000–2011) ftp://ftp.ntsg.umt.edu/pub/MODIS/Mirror/MOD16/. Accessed 24 April 2013

Palmer AR, Weideman CI (2011) Exploring trends in evapotranspiration in the KNP: towards a water use efficiency model for rangeland production in semi-arid savannas. Proceedings of the IXth International Rangeland Congress, Rosario, Argentina, 2–8 April 2011

Palmer AR, Yunusa I (2011) Biomass production and water use efficiency of arid rangelands in the Riemvasmaak Rural Area, Northern Cape, South Africa. J Arid Environ 75:1223–1227

Scanlon BR, Healy RW, Cook PG (2002) Choosing appropriate techniques for quantifying groundwater recharge. Hydrol J 10:18–39

Scanlon BR, Keese KE, Flint AL, Flint LE, Gaye CB, Edmunds WM, Simmers I (2006) Global synthesis of groundwater recharge in semiarid and arid regions. Hydrol Process 20:3335–3370

Schulze RE, Lynch SD (2007) Annual precipitation. In: Schulze RE (ed) South African atlas of climatology and agrohydrology. Water Research Commission, Pretoria, South Africa

Smit PJ (1977) Die Geohidrologie in die opvanggebied van die Moloporivier in die Noordelike Kalahari [The geohydrology in the catchment area of the Molopo River in the northern Kalahari], vol I. PhD Thesis, University of the Free State, South Africa

Szilagyi J, Zlotnik VA, Gates JB, Jozsa J (2011) Mapping mean annual groundwater recharge in the Nebraska Sand Hills, USA. Hydrogeol J 19:1503–1513

Szilagyi J, Kovacs A, Jozsa (2012) Remote-sensing based groundwater recharge estimates in the Danube-Tisza sand plateau region of Hungary. J Hydrol Hydromech 60:64–72

Thomas DSG, Shaw PA (1991) The Kalahari environment. Cambridge University Press, Cambridge

Timmerman LRA (1985a) Possibilities for the development of groundwater from the Cenozoic sediments in the lower Berg River Region. Report no. GH3374, Dept. of Water Affairs, Cape Town, South Africa. Available online at http://www.dwa.gov.za/ghreport/. Accessed 24 April 2013

Timmerman LRA (1985b) Preliminary report on the Cenozoic sediments of part of the Coastal Plain between the Berg River and Eland's Bay. Report no. GH3370, Dept. of Water Affairs, Cape Town, South Africa. Available online at http://www.dwa.gov.za/ghreport/. Accessed 24 April 2013

Timmerman LRA (1986) Sandveld region: possibilities for the development of a groundwater supply scheme from a primary aquifer northwest of Graafwater. Report no. GH3471, Dept. of Water Affairs, Cape Town, South Africa. Available online at http://www.dwa.gov.za/ghreport/. Accessed 24 April 2013

Van den Berg EC, Plarre C, Van den Berg HM, Thompson MW (2008) The South African National Land Cover 2000. Report GW/A/2008/86. Agricultural Research Council-Institute for Soil, Climate and Water, Pretoria, South Africa

Van Straten OJ (1955) The geology and groundwater of the Ghanzi cattle route. Bechuanaland Protectorate Geol Survey, Lobatse, Botswana, pp 28–39. Available online at http://www.bgs.ac.uk/sadcreports/botswana1955gsannualreport.pdf. Accessed 24 April 2013

Vandoolaeghe MAC, Bertram E (1982) Atlantis Grondwatersisteem: Herevaluasie van Versekerde Lewering. Report no. GH3222, Dept. of Water Affairs, Cape Town, South Africa. Available online at http://www.dwa.gov.za/ghreport/. Accessed 24 April 2013

Xu Y, Beekman HE (eds) (2003) Groundwater recharge estimation in Southern Africa. UNESCO IHP Series No. 64, UNESCO, Paris